Fluctuation-Corrected Phase Diagrams for Diblock Copolymer Melts

Mark W. Matsen,[1,2,3,*] Tom M. Beardsley,[1] and James D. Willis[2]

[1] *Department of Chemical Engineering,*
University of Waterloo, Waterloo, Ontario N2L 3G1, Canada

[2] *Department of Physics & Astronomy,*
University of Waterloo, Waterloo, Ontario N2L 3G1, Canada

[3] *Waterloo Institute for Nanotechnology,*
University of Waterloo, Waterloo, Ontario N2L 3G1, Canada

Abstract

New developments in field-theoretic simulations (FTSs) are used to evaluate fluctuation corrections to the self-consistent field theory (SCFT) of diblock copolymer melts. Conventional simulations have been limited to the order-disorder transition (ODT), whereas FTSs allow us to evaluate complete phase diagrams for a series of invariant polymerization indices. The fluctuations stabilize the disordered phase, which shifts the ODT to higher segregation. Furthermore, they stabilize the network phases at the expense of the lamellar phase, which accounts for the presence of the Fddd phase in experiments. We hypothesize that this is due to an undulation entropy that favors curved interfaces.

(May 20, 2023)

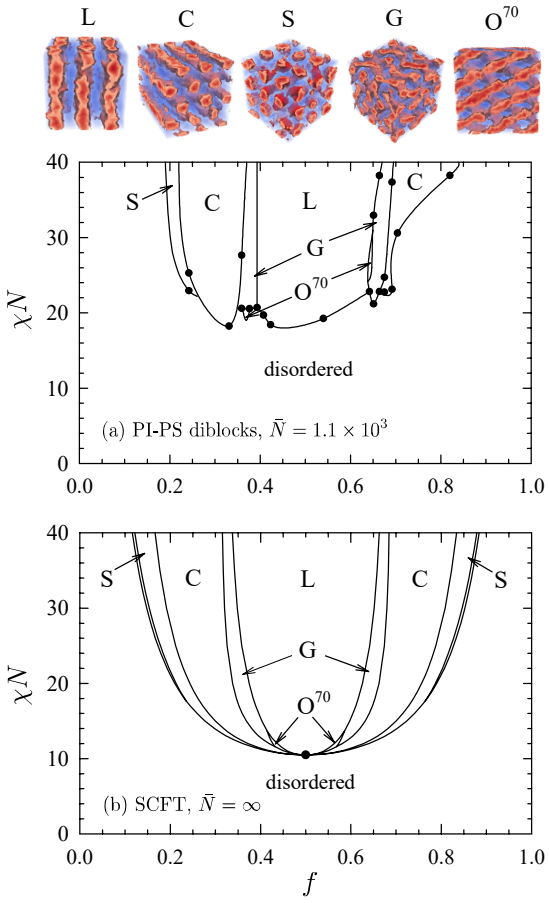


FIG. 1. (a) Experimental phase diagram for PI-PS diblock copolymers [8–12] and (b) theoretical phase diagram calculated using SCFT [17]. The images at the top show the domain structure of the ordered phases obtained from FTSs.

Block copolymers are a special class of polymers, where the chain is divided into chemically-distinct blocks. These molecules have received tremendous attention due to their intriguing self-assembly behavior and applications [1–3]. They also serve as a model system for studying lyotropic liquid crystals [4, 5] and biological membranes [6, 7], because of their theoretical tractability. The generic behavior of block copolymers is well captured by the simple AB diblock architecture, involving a block of fN A-type segments joined to a block of $(1-f)N$ B-type segments. Driven by a general immiscibility of unlike components, a liquid (or melt) of diblock copolymers self-assembles into A- and B-rich domains. The domains remain microscopic in size due to the connectivity of the blocks, resulting in periodically-ordered microstructures.

Figure 1(a) shows a phase diagram for polyisoprene-polystyrene (PI-PS) diblock copoly-

mer melts [8–12]. The stable microstructures include the classical lamellar (L), cylindrical (C), and spherical (S) phases as well as two complex network phases referred to as gyroid (G) and Fddd (O^{70}). The geometry is controlled primarily by the diblock composition, f, and the degree of order by the product χN, where χ is the Flory-Huggins parameter specifying the immiscibility of A and B segments.

One remarkable property of block copolymers is that their behavior becomes universal at large N [13–15], once the atomistic details are small relative to the size of the polymers, $R_0 = aN^{1/2}$; for simplicity, we assume equal statistical lengths, a, for the A and B segments. If the universality holds, then even coarse-grained models are sufficient for quantitative predictions. The standard choice is the Gaussian-chain model (GCM) [16], where the system is treated as an incompressible melt of thin elastic threads. In this model, the A and B segments interact by contact forces with a strength proportional to χ.

The phase behavior of the standard GCM is generally well described by mean field or rather self-consistent field theory (SCFT). Indeed, the SCFT phase diagram [17], shown in Fig. 1(b), exhibits the same sequence of phases observed in experiments. In fact, SCFT [18] predicted the stability of gyroid [19, 20] over a perforated-lamellar phase [21] well before experiments demonstrated so [22, 23]. Furthermore, SCFT [24] predicted the Fddd phase years before it was actually discovered [11, 12]. However, there is one important difference in the topology of the phase diagrams. Experiments observe direct ODTs with the various ordered phases, whereas SCFT predicts that the spherical phase extends down to a critical point at $f = 0.5$ and $\chi N = 10.495$, separating the other ordered phases from the disordered phase. This difference is attributed to fluctuation effects, which are controlled by the invariant polymerization index

$$\bar{N} = a^6 \rho_0^2 N, \tag{1}$$

where ρ_0 is the segment density. SCFT neglects fluctuations and thus corresponds to $\bar{N} \to \infty$ [25], whereas $\bar{N}$ generally varies from 10^2 to 10^4 in experiments [10]. In the case of the PI-PS diblocks, $\bar{N} \approx 1100$.

In a seminal 1987 paper by Fredrickson and Helfand [26], the fluctuation correction was estimated using a Landau-Brazovskii theory. They showed that fluctuations expand the disordered region, causing direct transitions with each of the ordered phases. However, the approximations involved begin to break down for $\bar{N} \lesssim 10^{10}$, and thus are inaccurate for experimental conditions. In any case, simulations [27–29] confirmed the direct transitions

some time ago, but only recently has the position of the ODT been accurately calibrated. For symmetric diblocks ($f = 0.5$), it occurs at

$$(\chi N)_{\mathrm{ODT}} = 10.495 + 41.0\bar{N}^{-1/3} + 123.0\bar{N}^{-0.56}. \tag{2}$$

The first term is the SCFT prediction, the second is the correction of Fredrickson and Helfand, and the third is an empirical correction from simulations [14]. Further simulations [30] at other compositions, f, reveal similar shifts in the L- and C-disorder transitions.

It is not clear what happens to the order-order transitions (OOTs). The Landau-Brazovskii theory predicts a direct G-disorder transition consistent with experiment [31], but it also predicts the Fddd phase to be destroyed by fluctuations at experimentally relevant values of $\bar{N}$ [32]. Unfortunately, simulations are hindered by the fact that the simulation box needs to be commensurate with the equilibrium periodicity of an ordered phase, which precludes the use of a single box size. Nevertheless, Delaney and Fredrickson [33] have managed to compare ordered phases between different boxes using field-theoretic simulations (FTSs), which are capable of calculating free energies with sufficient precision to discern the relative stabilities [28, 34]. However, the fluctuations in their FTSs were insufficient to produce a direct G-disorder transition, and yet they still destroyed the Fddd phase. It has been suggested [35, 36] that these inconsistencies with experiment may be due to long-range interactions introduced in order to remove an ultraviolet (UV) divergence from the standard GCM [37]. Our aim in this Letter is to investigate the universal behavior in the large-N regime. We again apply FTSs, but this time retaining the contact forces of the standard GCM, and instead removing the UV divergence by renormalizing χ. The foundations underpinning our FTSs and the technical details of the implementation can be found in Ref. 38.

In polymer field theory [39, 40], the particle-based GCM is converted to a field-based version. The resulting Hamiltonian, $H[W_-, W_+]$, takes the form

$$\frac{H_f}{nk_BT} = -\ln Q + \frac{\chi_b N}{4} + \frac{N}{V}\int\left(\frac{W_-^2}{\chi_b} - W_+\right)d\mathbf{r}, \tag{3}$$

where V is the volume of the system, $n = \rho_0 V/N$ is the total number of molecules, and χ_b is the *bare* interaction parameter. The $Q[W_-, W_+]$ is a partition function for a single diblock, where the A and B segments are acted upon by the fields $W_A(\mathbf{r}) = W_+(\mathbf{r}) + W_-(\mathbf{r})$ and $W_B(\mathbf{r}) = W_+(\mathbf{r}) - W_-(\mathbf{r})$, respectively. SCFT approximates the free energy by $F =$

$H_f[w_-, w_+]$, where $w_-(\mathbf{r})$ and $w_+(\mathbf{r})$ denote the saddle-point of the Hamiltonian, whereas FTSs simply simulate $H_f[W_-, W_+]$. However, there is the complication that $W_+(\mathbf{r})$ is imaginary valued, which Fredrickson and co-workers handle by performing complex-Langevin FTSs [28, 33, 41]. Given that the $W_-(\mathbf{r})$ fluctuations are dominant [38], we instead invoke a partial saddle-point approximation for $W_+(\mathbf{r})$ [42–45]. It turns out that $w_+(\mathbf{r})$ is real, which therefore allows us to simulate $H[W_-, w_+]$ using conventional Langevin dynamics. We also switch from continuous to discrete chains with $N = 90$ monomers, so as to remove a source of numerical inaccuracy. The computer code used for our FTSs is available from Ref. 38. Note, however, that we now increment the Langevin dynamics using the Leimkuhler-Matthews algorithm, which speeds up the FTSs more than $10\times$ relative to the predictor-corrector algorithm [46].

The calculations are performed in $L_x \times L_y \times L_z$ orthorhombic boxes with periodic boundary conditions. In order to represent the fields, the boxes are overlayed with $m_x \times m_y \times m_z$ grids of uniform spacing, $\Delta_\nu = L_\nu/m_\nu$, in the $\nu = x$, y, and z directions. Hence, each grid point corresponds to a finite volume of $V_{\text{cell}} = V/M$, where $V = L_x L_y L_z$ and $M = m_x m_y m_z$. In SCFT, an acceptable accuracy is readily achieved by choosing a sufficiently fine grid, but in FTSs, one also has to contend with the UV divergence. Although the model defines the interactions as contact forces, in practice, the range is dictated by the grid spacings, Δ_ν. Consequently, the number of intermolecular interactions decreases as $V_{\text{cell}} \to 0$, causing a reduction in segregation.

Fortunately, the polymer field theory appears to be renormalizable [47]. As such, the UV divergence can be removed by expressing results in terms of a renormalized or rather *effective* interaction parameter

$$\chi = z_\infty \chi_b + c_2 (z_\infty \chi_b)^2 + c_3 (z_\infty \chi_b)^3 + \cdots \ , \tag{4}$$

where z_∞ is the relative number of intermolecular contacts in the limit of $\chi_b \to 0$ and $N \to \infty$, which can be calculated analytically [36, 40]. The remaining coefficients, c_p for $p = 2, 3, ...$, are determined by a Morse calibration [14, 48, 49], where the structure function, $S(k)$, for disordered melts of symmetric diblock copolymer is fit to renormalized one-loop (ROL) predictions [50].

Figure 2 displays our phase diagrams for $\bar{N} = 10^6$, 10^5, and 10^4. They are plotted in terms of the effective χ in Eq. (4), where the coefficients, $c_2 = 0.012$, 0.041, and 0.21, respectively,

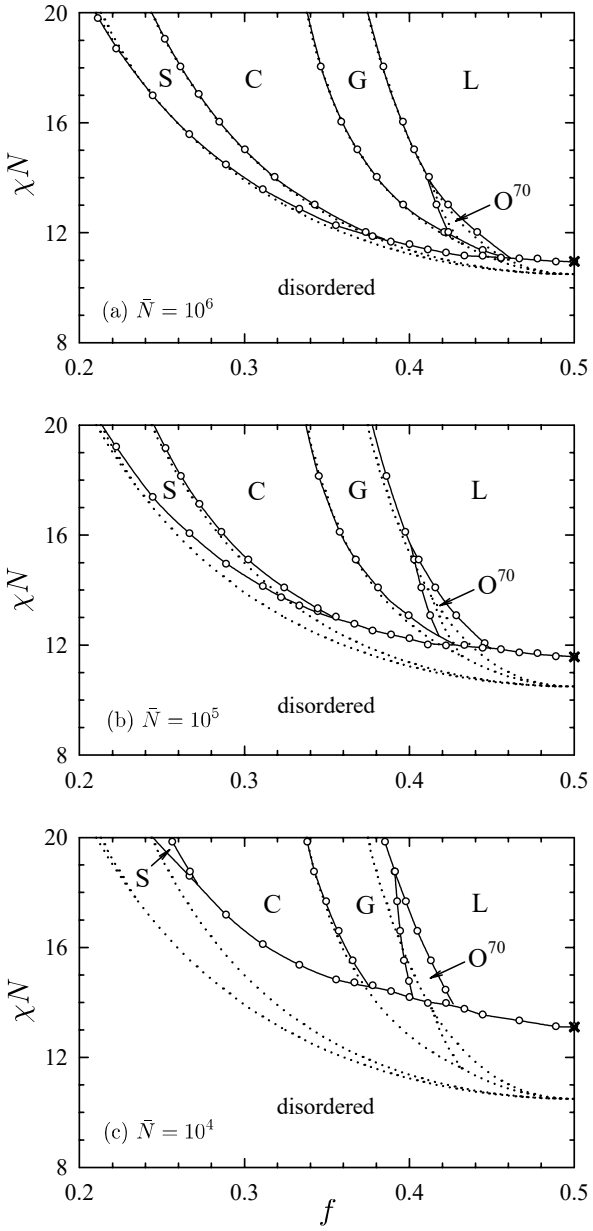


FIG. 2. Phase diagrams for (a) $\bar{N} = 10^6$, (b) $\bar{N} = 10^5$, and (c) $\bar{N} = 10^4$, calculated using FTS. Circles denote the FTS data points, crosses show predictions of Eq. (2), and dotted curves compare the SCFT phase boundaries from Fig. 1(b).

are evaluated as described in Ref. 36; given the large values of $\bar{N}$, we set $c_3 = c_4 = \cdots = 0$. Note that the Morse calibration not only corrects for the UV divergence, but also accounts for the switch from continuous to discrete chains [36]. This is evident by the fact that the FTS results converge to the SCFT phase diagram of the standard GCM in Fig. 1(b) (dotted curves) with increasing $\bar{N}$.

The ODTs in Fig. 2 are located by monitoring the disappearance of scattering peaks in the structure function, $S(k)$, of the ordered phases with decreasing χ, as demonstrated in Ref. 35. The accuracy of this procedure has been validated by well-tempered metadynamics [51]. Note that the periodicity of the ordered phases is provided by SCFT, as previously justified [35, 36, 51]. To avoid finite-size effects, the simulations for the L, C, S, G, and O^{70} phases are performed in relatively large boxes containing 3, 6, 27, 8, and 8 unit cells, respectively, as depicted in Fig. 1. The fact that our ODTs for $f = 0.5$ agree with Eq. (2) adds to the preceding evidence [43, 45, 52] that the partial saddle-point approximation is accurate for the large values of $\bar{N}$ considered here.

To obtain the OOTs, we evaluate the free energies of the ordered phases with thermodynamic integration (TI) [28, 36]. This involves simulating the composite Hamiltonian,

$$H = \lambda H_f + (1 - \lambda) H_{\mathrm{ec}}, \tag{5}$$

which combines the polymer Hamiltonian in Eq. (3) with the Hamiltonian for an Einstein crystal of harmonic oscillators,

$$\frac{H_{ec}}{nk_BT} = \frac{N}{V\chi_b}\int (W_- - W_{\mathrm{ec}})^2 d\mathbf{r}. \tag{6}$$

The reference field, $W_{\mathrm{ec}}(\mathbf{r})$, is generally set to a previously equilibrated configuration of the ordered phase for similar system parameters. During the simulation, H_f and H_{ec} are sampled as λ is gradually incremented from 0 to 1 in steps of $d\lambda$. Once the simulation is complete, the free energy is given by [36]

$$F = \int_0^1 (H_f - H_{\mathrm{ec}}) d\lambda. \tag{7}$$

Our OOTs are located by linearly interpolating between free energies evaluated at equal values of χN on opposing sides of the transition; recall that $f = N_A/N$ is restricted to discrete values. Because of the computational cost of the TIs, we reduce the boxes of the L, C, S, G, and O^{70} phases to 3, 4, 8, 1, and 2 unit cells, respectively. Even still, we expect minimal finite-size effects (see Refs. 36 and 51). The step sizes in our TIs are generally small enough ($d\lambda \sim 10^{-5}$-10^{-6}) to ensure accurate phase boundaries on the scale of our plots. The only exception is the G-O^{70} boundary at $\bar{N} = 10^4$, where statistical inaccuracies become comparable to the symbol size, as a result of the large fluctuations and the structural similarity of the two network phases.

Because the phases of an OOT need to be simulated in different boxes, they will inevitably require different grid resolutions. Although the renormalization of χ_b accurately accounts for this difference, small imperfections do become significant when evaluating free energies to the high precision required to locate OOTs. Fortunately, we are saved by a recent discovery [36] that the inaccuracy in the renormalization vanishes as the difference in V_{cell} approaches zero. Given that V_{cell} can be varied arbitrarily for phases with one or more directions of translational invariance (e.g., the disordered, L, and C phases), it is usually possible to choose boxes with identical cell volumes. In our case, the only exception is the G-O^{70} boundary. Nevertheless, we manage to find boxes with V_{cell} values matching to $\lesssim 2\%$. Furthermore, we are able to correct for the slight mismatch by examining the effect of V_{cell} on the free energy of the lamellar phase, as proposed in Ref. 36. Even for $\bar{N} = 10^4$, the effect proves to be small.

The validity of our phase diagrams is bolstered by the sensible evolution from SCFT as $\bar{N}$ becomes finite. At our largest $\bar{N} = 10^6$, the shift in the ODT is only appreciable near the mean-field critical point, exactly as predicted by the Landau-Brazovskii calculation of Fredrickson and Helfand [26]. Interestingly, the Fddd region shifts toward higher segregation and the G region expands toward the lamellar region. Naturally, the fluctuation effects should increase monotonically as $\bar{N}$ is reduced, but nevertheless the degree to which the Fddd region shifts upward is remarkable.

Even though $\bar{N} = 10^4$ is still relatively large compared to typical experiments, the fluctuation shift of the ODT is considerable, as it must be. The experimental phase diagram in Fig. 1(a) indicates that the complex-phase channel is pushed up to $(\chi N)_{\text{ODT}} \approx 20$ for $\bar{N} = 1.1 \times 10^3$. Based on improved estimates of χ [53], the shift is actually somewhat larger. Indeed, recent simulations [30] suggest an ODT of $(\chi N)_{\text{ODT}} \approx 25$. In any case, these values far exceed the top of the Fddd region in the SCFT phase diagram, located at $\chi N = 13.7$ in Fig. 1(b) [24, 54]. Thus, the large upward shift of the Fddd region in Fig. 2 is, in fact, necessary to account for its survival in PI-PS diblock copolymer melts [11, 12].

We attribute the failure of the Landau-Brazovskii calculation to predict a stable Fddd phase for $\bar{N} \lesssim 10^4$ [32] to the truncation of large wavevectors, which prevents small-scale undulations of the internal interfaces. The entropy of the interfacial undulations is known to favor curved interfaces in lytopic liquid crystals [55], and the same has been hypothesized for block copolymer melts [56]. This would account for the shift of the network phases

toward the L region. The lack of a significant shift of their boundaries with the C region could be explained by the relatively close match in interfacial curvatures [57]. Naturally, the interfaces of the S phase are significantly more curved than those of the C phase, and accordingly the S-C boundary shifts toward the C region. Thus, this hypothesis does, in fact, fit with our observations.

Given the relatively large $N = 90$, our phase diagrams should be universal. Indeed, the ODTs at $f = 0.5$ are perfectly consistent with Eq. (2). The significance is that all other models will exhibit identical phase diagrams, once N is large enough to produce a sufficient separation between the length scales of the microscopic (i.e., atomistic) details, which are independent of N, and the size of the polymers, which increases as $R_0 = aN^{1/2}$. In this regime, the dependence on the microscopic details, no matter how many extra parameters that might entail, can be completely adsorbed into the effective χ. For instance, the phase diagrams of Delaney and Fredrickson [33] should become identical to ours if the range of their interactions was small relative to R_0, although not necessarily zero. Even the dependence on the particular shape of their interaction potential would be adsorbed into χ. This is also, in principle, true of experiments, but it should be noted that our phase diagrams are specific to monodisperse diblock copolymers with equal segment lengths. Thus, even if the PI-PS diblocks conform to the large-N regime, there would still be some differences due to polydispersity and conformational asymmetry.

Now that we are able to access the universal behavior of the large-N regime, there are many other block copolymer systems that could be investigated. One of the main advantages of FTSs is their immense versatility. In particular, they can handle complicated polymeric architectures with a minimal increase in computational effort relative to that of the simple diblock [58, 59], which is not the case for conventional simulations. Furthermore, they can be adapted to a variety of ensembles [60–62], which is particularly useful when dealing with blends. For AB-type systems [17], the modifications to the algorithm are relatively simple [38]. The extension to three or more chemically-distinct components (e.g., ABC-type systems) is also possible, although less trivial [63].

In summary, we have calculated fluctuation-corrected phase diagrams for diblock copolymer melts calibrated with respect to the standard Gaussian-chain model (GCM). Consistent with experiments, we find direct G-disorder transitions for $\bar{N} \lesssim 10^4$. Furthermore, we predict a considerable stabilization of the Fddd phase, sufficient to account for its presence

in PS-PI melts of $\bar{N} \approx 1.1 \times 10^3$. This suggests that the entropic preference for curved interfaces in lytopic liquid crystals [55] also extends to block copolymers, and likely beyond. After 35 years since Fredrickson and Helfand [26] provided the first insights into fluctuation effects in block copolymer melts, we now have accurate predictions for the complete phase diagram in the universal regime of large N. Given the versatility of FTSs, they are destined to become a powerful means of investigating fluctuation effects in a wide-range of other block copolymer systems, not to mention lytropic liquid crystals and biological membranes. Admittedly, there will need to be further testing of the partial saddle-point approximation to determine the full range of applicability.

We are grateful to Glenn Fredrickson, Dave Morse, and Russell Spencer for valuable discussions. This work was supported by NSERC of Canada, and computer resources were provided by the Digital Research Alliance of Canada.

* Corresponding author.
mwmatsen@uwaterloo.ca

[1] F. S. Bates, Polymer-Polymer Phase Behavior, Science **251**, 898–905 (l991).

[2] F. S. Bates and G. H. Fredrickson, Block copolymers-designer soft materials, Physics Today **52**, 32–38 (2000).

[3] F. S. Bates, M. A. Hillmyer, T. P. Lodge, C. M. Bates, and G. H. Fredrickson, Multiblock polymers: Panacea or Pandora's box? Science **336**, 434–440 (2012).

[4] W. B. Lee, R. Mezzenga, G. H. Fredrickson, Anomalous Phase Sequences in Lytropic Liquid Crystals, Phys. Rev. Lett. **99**, 187801 (2007).

[5] W. B. Lee, R. Mezzenga, G. H. Fredrickson, Self-consistent field theory for lipid-based liquid crystals: Hydrogen bonding effect, J. Chem. Phys. **128**, 074504 (2008).

[6] M. Müller, K. Katsov, and M. Schick, Biological and synthetic membranes: What can be learned from a course-grained description? Phys. Reports **434** 113–176 (2006).

[7] C. L. Ting, D. Appelö, and Z.-G. Wang, Minimum energy path to membrane pore formation and rupture, Phys. Rev. Lett. **106**, 168101 (2011).

[8] S. Förster, A. K. Khandpur, J. Zhao, F. S. Bates, I. W. Hamley, A. R. Ryan, and W. Bras, Complex Phase Behavior of Polyisoprene–Polystyrene Diblock Copolymers Near the Order–

Disorder Transition, Macromolecules **27**, 6922–6935 (1994).

[9] S. Förster, A. K. Khandpur, J. Zhao, F. S. Bates, I. W. Hamley, A. R. Ryan, and W. Bras, Polyisoprene–Polystyrene Diblock Copolymer Phase Diagram near the Order–Disorder Transition, Macromolecules **28**, 8796–8806 (1995).

[10] F. S. Bates, M. F. Schulz, A. K. Khandpur, S. Förster, J. H. Rosedale, K. Almdal, and K. Mortensen, Fluctuations, Conformational Asymmetry and Block Copolymer Phase Behaviour, Faraday Discuss. **98**, 7–18 (1994).

[11] M. Takenaka, T. Wakada, S. Akasaka, S. Nishitsuji, K. Saijo, H. Shimizu, M. I. Kim, and H. Hasegawa, Orthorhombic Fddd Network in Diblock Copolymer Melts, Macromolecules **40**, 4399–4402 (2007).

[12] Y.-C. Wang, K. Matsuda, M. I. Kim, A. Miyoshi, S. Akasaka, S. Nishitsuji, K. Saijo, H. Hasegawa, K. Ito, T. Hikima, and M. Takenaka, Fddd Phase Boundary of Polystyrene-block-polyisoprene Diblock Copolymer Melts in the Polystyrene-Rich Region, Macromolecules **48**, 2211–2216 (2015).

[13] J. Glaser, J. Qin, P. Medapuram, M. Müller, and D. C. Morse, Test of a scaling hypothesis for the structure factor of disordered diblock copolymer melts, Soft Matter **113**, 11310–11317 (2012).

[14] J. Glaser, P. Medapuram, T. M. Beardsley, M. W. Matsen, and D. C. Morse, Universality of block copolymer melts, Phys Rev. Lett. **113**, 068302 (2014).

[15] T. M. Beardsley and M. W. Matsen, Universality between experiment and simulation of a diblock copolymer melt. Phys. Rev. Lett. **117**, 217801 (2016).

[16] M. W. Matsen, The standard Gaussian model for block copolymer melts. J. Phys.: Condens. Matter **14**, R21–R47 (2002).

[17] M. W. Matsen, Effect of architecture on the phase behavior of AB-type block copolymer melts, Macromolecules **45**, 2161–2165 (2012).

[18] M. W. Matsen and M. Schick, Stable and unstable phases of a diblock copolymer melt, Phys. Rev. Lett. **72**, 2660-2663 (1994).

[19] D. A. Hajduk, P. E. Harper, S. M. Gruner, C. C. Honeker, G. Kim, and E. L. Thomas, The Gyroid: A New Equilibrium Morphology in Weakly Segregated Diblock Copolymers, Macromolecules **27**, 4063–4075 (l994).

[20] M. F. Schulz, F. S. Bates, K. Almdal, and K. Mortensen, Epitaxial Relationship for Hexagonal-

to-Cubic Phase Transition in a Block Copolymer Mixture. Phys. Rev. Lett. **73**, 86–89 (1994).

[21] I. W. Hamley, K. A. Koppi, J. H. Rosedale, and F. S. Bates, K. Almdal, and K. Mortensen, Hexagonal Mesophases between Lamellae and Cylinders in a Diblock Copolymer Melt, Macromolecules **26**, 5959–5970 (1993).

[22] D. A. Hajduk, H. Takenouchi, M. A. Hillmyer, F. S. Bates, M. E. Vigild, and K. Almdal, Stability of the Perforated Layer (PL) Phase in Diblock Copolymer Melts, Macromolecules **30**, 3788-3795 (1997).

[23] M. E. Vigild, K. Almdal, K. Mortensen, I. W. Hamley, J. P. A. Fairclough, and A. J. Ryan, Transformations to and from the Gyroid Phase in a Diblock Copolymer, Macromolecules **31**, 5702–5716 (1998).

[24] C. T. Tyler and D. C. Morse, Orthorhombic Fddd Network in Triblock and Diblock Copolymer Melts, Phys. Rev. Lett. **94**, 208302 (2005).

[25] J. Qin and D. C. Morse, Fluctuations in Symmetric Diblock Copolymers: Testing Theories Old and New, Phys. Rev. Lett. **108**, 238301 (2012).

[26] G. H. Fredrickson and E. Helfand, Fluctuation effects in the theory of microphase separation in block copolymers, J. Chem. Phys. **87**, 697–705 (1987).

[27] M. W. Matsen, G. H. Griffiths, R. A. Wickham, and O. N. Vassiliev, Monte Carlo phase diagram for diblock copolymer melts, J. Chem. Phys. **124**, 024904 (2006).

[28] E. M. Lennon, K. Katsov, and G. H. Fredrickson, Free Energy Evaluation in Field-Theoretic Polymer Simulations, Phys. Rev. Lett. **101**, 138302 (2008).

[29] T. M. Beardsley and M. W. Matsen, Monte Carlo phase diagram for diblock copolymer melts, Eur. Phys. J. E **32**, 255–264 (2010).

[30] T. Ghasimakbari and D. C. Morse, Order-Disorder Transitions and Free Energies in Asymmetric Diblock Copolymers, Macromolecules **53**, 7399–7409 (2020).

[31] I. W. Hamley and V. E. Podneks, On the Landau-Brazovskii theory for block copolymer melts, Macromolecules **30**, 3701–3703 (1997).

[32] B. Miao and R. A. Wickham, Fluctuation effects and the stability of the Fddd network phase in diblock copolymer melts, J. Chem. Phys. **128**, 054902 (2008).

[33] K. T. Delaney and G. H. Fredrickson, Recent Developments in Fully Fluctuating Field-Theoretic Simulations of Polymer Melts and Solutions, Macromolecules **120**, 7615 (2016).

[34] G. H. Fredrickson and K. T. Delaney, Direct free energy evaluation of classical and quan-

tum many-body systems via field-theoretic simulation, Proc. Natl. Acad. Sci. U. S. A. **119**, e2201804119 (2022).

[35] T. M. Beardsley and M. W. Matsen, Fluctuation correction for the order-disorder transition of diblock polymer melts, J. Chem. Phys. **154**, 124902 (2021).

[36] M. W. Matsen, T. M. Beardsley, and J. D. Willis, Accounting for the ultra-violet divergence in field-theoretic simulations of block copolymer melts, J. Chem. Phys. **158**, 044904 (2023).

[37] M. Olvera de la Cruz, S. F. Edwards, and I. C. Sanchez, Concentration Fluctuations in Polymer Blend Thermodynamics, J. Chem. Phys. **89**, 1704–1708 (1988).

[38] M. W. Matsen and T. M. Beardsley, Field-theoretic simulations for block copolymer melts using the partial saddle-point approximation, Polymers **13**, 2437 (2021).

[39] G. H. Fredrickson, V. Ganesan, and F. Drolet, Field-Theoretic Computer Simulation Methods for Polymers and Complex Fluids, Macromolecules **35**, 16–39 (2002).

[40] M. W. Matsen, Field theoretic approach for block polymer melts: SCFT and FTS, J. Chem. Phys. **152**, 110901 (2020).

[41] V. Ganesan and G. H. Fredrickson, Field-theoretic polymer simulations, Eurphys. Lett. **55**, 814–820 (2001).

[42] E. Reister, M. Müller, and K. Binder, Spinodal decomposition in a binary polymer mixture: Dynamic self-consistent-field theory and Monte Carlo simulations, Phys. Rev. E **64**, 041804 (2001).

[43] D. Düchs, V. Ganesan, G. H. Fredrickson, and F. Schmid, Fluctuation Effects in Ternary AB + A + B Polymeric Emulsions, Macromolecules **36**, 9237–9248 (2003).

[44] P. Stasiak and M. W. Matsen, Monte Carlo field-theoretic simulations for melts of symmetric diblock copolymer, Macromolecules **46**, 8037 (2013).

[45] T. M. Beardsley, R. K. W. Spencer, and M. W. Matsen, Computationally efficient field-theoretic simulations for block copolymer melts, Macromolecules **52**, 8840–8848 (2019).

[46] B. Vorselaars, Efficient Langevin and Monte Carlo sampling algorithms: The case of field-theoretic simulations, J. Chem. Phys. **158**, 114117 (2023).

[47] P. Grzywacz, J. Qin, and D. C. Morse, Renormalization of the one-loop theory of fluctuations in polymer blends and diblock copolymer melts, Phys. Rev. E **76**, 061802 (2007).

[48] J. Qin and D. C. Morse, Renormalized One-Loop Theory of Correlations in Polymer Blends, J. Chem. Phys. **130**, 224902 (2009).

[49] J. Glaser, P. Medapuram, and D. C. Morse, Collective and Single-Chain Correlations in Disordered Melts of Symmetric Diblock Copolymers: Quantitative Comparison of Simulations and Theory, Macromolecules **47**, 851–869 (2014).

[50] J. Qin, P. Grzywacz, and D. C. Morse, Renormalized one-loop theory of correlations in disordered diblock copolymers, J. Chem. Phys. **135**, 084902 (2011).

[51] T. M. Beardsley and M. W. Matsen, Well-tempered metadynamics applied to field-theoretic simulations of diblock copolymer melts, J. Chem. Phys. **157**, 114902 (2022).

[52] A. Alexander-Katz and G. H. Fredrickson, Diblock copolymer thin films: A field-theoretic simulation study. Macromolecules **40**, 4075–4087 (2007).

[53] J. D. Willis, T. M. Beardsley, and M. W. Matsen, Simple and accurate calibration of the Flory-Huggins interaction parameter, Macromolecules **53**, 9973–9982 (2020).

[54] M. W. Matsen, Fast and accurate SCFT calculations for periodic block-copolymer morphologies using the spectral method with Anderson mixing, Eur. Phys. J. E **30**, 361–369 (2009).

[55] D. C. Morse, Entropy and fluctuations of monolayers, membranes, and microemulsions, Curr. Opin. Colloid Interface Sci. **2**, 365–372 (1997).

[56] M. Yadav, F. S. Bates, and D. C. Morse, Network Model of the Disordered Phase in Symmetric Diblock Copolymer Melts. Phys. Rev. Lett. **121**, 127802 (2018).

[57] M. W. Matsen and F. S. Bates, Origins of complex self-assembly in block copolymers. Macromolecules **29**, 7641–7644 (1996).

[58] Y. X. Liu, K. T. Delaney, and G. H. Fredrickson, Field-Theoretic Simulations of Fluctuation-Stabilized Aperiodic Bricks-and-Mortar Mesophase in Miktoarm Star Block Copolymer/Homopolymer Blends, Macromolecules **50**, 6263–6272 (2017).

[59] R. K. W. Spencer and M. W. Matsen, Field-theoretic simulations of bottlebrush copolymers, J. Chem. Phys. **149**, 184901 (2018).

[60] R. K. W. Spencer and M. W. Matsen, Fluctuation effects in blends of A+B homopolymers with AB diblock copolymer, J. Chem. Phys. **148**, 204907 (2018).

[61] R. A. Riggleman and G. H. Fredrickson, Field-theoretic simulations in the Gibbs ensemble, J. Chem. Phys. **132**, 024104 (2010).

[62] J. P. Koski and R. A. Riggleman, Field-theoretic simulations of block copolymer nanocomposites in a constant interfacial tension ensemble, J. Chem. Phys. **146**, 164903 (2017).

[63] D. Düchs, K. T. Delaney, and G. H. Fredrickson, A multi-species exchange model for fully

fluctuating polymer field theory simulations. J. Chem. Phys. **36**, 174103 (2014).